VIP Organic Electronics Very Important Paper

Deutsche Ausgabe: DOI: 10.1002/ange.201504190
Internationale Ausgabe: DOI: 10.1002/anie.201504190

Head-to-Tail Zig-Zag Packing of Dipolar Merocyanine Dyes Affords High-Performance Organic Thin-Film Transistors**

*Aifeng Lv, Matthias Stolte, and Frank Würthner**

Abstract: *Attachment of bulky substituents at both thiophene donor (D) and thiazole acceptor (A) heterocycles of a dipolar ($\mu_g = 10.4$ D) D-π-A merocyanine dye affords a more than 1 Å expansion of the common antiparallel supramolecular dimer motif in the solid state, enabling very close π-contacts (3.36 Å) to two other neighbor molecules on each of the two remaining π-faces. This unusual packing motif leads to three-dimensional percolation pathways for hole transport and affords thin-film transistors with mobility up to 0.64 $cm^2 V^{-1} s^{-1}$.*

Despite of their successful use in bulk heterojunction (BHJ) solar cells, dipolar donor–acceptor (DA) substituted π-systems are still not considered as ideal organic semiconductors. Thus, the success of merocyanines[1,2] and related DA dyes[3,4] in organic photovoltaics with power conversion efficiencies larger than 6% is more attributed to their outstanding absorption properties than to their hole transport capabilities. To shed more light onto the latter we initiated a research program on the use of highly dipolar merocyanine dyes in organic thin-film transistors (OTFTs)[5] and dedicated particular efforts on the elucidation of packing arrangements of merocyanine dyes in the solid state.[6,7] This work has so far reached to the following insights: The most common arrangement of merocyanine dyes in the solid state consists of antiparallel (centrosymmetric) dimers at close van-der-Waals distance ($d < 3.5$ Å), further packing of which is not easy to predict and may even lack additional π-contacts to neighbor molecules or show one-dimensional π-stacking, albeit with larger distances to the second neighbor (π-stack with alternating π-contacts, see Figure 1 a, left).[8,9] Closer inspection of a dozen of such packing motifs[10] suggests that most typically the closest neighbor interaction is optimized at the expense of the next neighbor. Accordingly one very close and electrostatically highly favorable contact is formed and any flexible substituents are directed towards the other face, thereby reducing the chance for close contacts to the other neighbor molecules as required for the most desirable two-dimensional brickwork or at least an equidistant one-dimensional columnar packing arrangement. As shown in our most previous study, this common packing arrangement may be changed by the presence of sterically demanding groups, for instance into two-dimensional brickwork-type slipped π-stacking motifs for derivatives based on the electron-donating 1-alkyl-3,3-dimethylindolin-2-ylidene ("Fischer base").[7] This class of molecules is indeed the so far only one among dipolar DA dyes that showed decent charge carrier mobility ($\mu_h = 0.18\ cm^2 V^{-1} s^{-1}$) in OTFTs. Therefore we wondered if the obviously highly favored but unsuitable antiparallel dimer packing could be overcome also for merocyanine dyes consisting of a monomethine-bridged aminothiophene donor and five-membered heterocyclic acceptor units[11] which so far all crystallized in the above-mentioned antiparallel dimer packing motif.[9] In accordance with our concept (see Figure 1 a) functionalization of the acceptor unit with bulky *tert*-butyl groups and replacement of alkyl chains at the amino group by more bulky phenyl units[12,13] indeed pushed the distance within the common antiparallel dimer motif significantly (by more than 1 Å compared to related dyes lacking such bulky substituents[9]) which afforded a fully accessible opposite π-face. Pleasingly, this arrangement triggered a hitherto unknown head-to-tail zig-zag packing motif with very close π-distances to two other neighbor

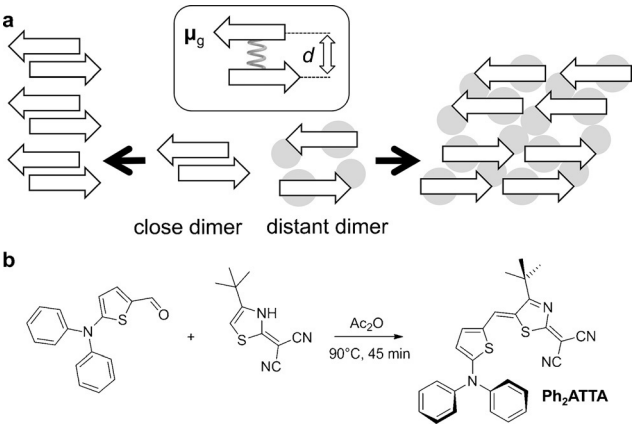

Figure 1. a) Crystal engineering concept for interconnected π-stacking arrangement (right) by expansion of the commonly observed close antiparallel π-dimer motif (left) with bulky groups. b) Synthesis of merocyanine **Ph_2ATTA**.

[*] Dr. A. Lv, Dr. M. Stolte, Prof. Dr. F. Würthner
Universität Würzburg, Institut für Organische Chemie and Center for Nanosystems Chemistry
Am Hubland 97074 Würzburg (Germany)
E-mail: wuerthner@chemie.uni-wuerzburg.de

[**] We thank Fabian Holzmeier for the synthesis of Ph_2ATTA during his practical course, Prof. Dr. Jens Pflaum and Dr. David Schmidt for thin-film XRD measurements, Dr. Marcel Gsänger for the single-crystal X-ray analysis, Alhama Arjona-Esteban and David Bialas for calculations, Dr. Vladimir Stepanenko for AFM measurements, and Ute Zschieschang and Hagen Klauk (MPI for Solid State Research, Stuttgart) for the preparation of TPA-modified wafers. Generous financial support by the Bavarian State Ministry of Science, Research, and the Arts for the Center for Nanosystems Chemistry in the framework of the Collaborative Research Network "Solar Technologies Go Hybrid" is gratefully acknowledged.

Supporting information for this article is available on the WWW under http://dx.doi.org/10.1002/anie.201504190.

molecules (3.36 Å) and enabled OTFTs with the so far highest charge carrier mobility of 0.64 $cm^2 V^{-1} s^{-1}$ among dipolar small molecule p-type semiconductors.

The new diphenyl**a**mino**t**hienyl-dicyanovinyl**thia**zol (**Ph_2ATTA**) (Figure 1b) was synthesized from 5-(diphenylamino)thiophene-2-carbaldehyde[14,15] and 2-(4-*tert*-butyl-5*H*-thiazol-2-ylidene)-malononitrile[11] by a condensation reaction in acetic anhydride in 35% yield (for details, see the Supporting Information). In addition to the standard chemical characterization by NMR spectroscopy, mass spectrometry, and elemental analysis, the molecular properties of **Ph_2ATTA** were elucidated by UV/Vis spectroscopy, electro-optical absorption spectroscopy, and cyclic voltammetry (for further details see the Supporting Information, Figure S1, S2, and S10 and Table S1). According to these studies **Ph_2ATTA** is a blue dye with an intense absorption band ($\lambda_{max} = 658$ nm; $\varepsilon_{max} = 68\,900\ M^{-1} cm^{-1}$ in chloroform), has a ground-state dipole moment of 10.4 D, and is reversibly oxidized at 0.49 V versus ferrocene/ferrocenium. The latter value suggests a HOMO energy level of −5.64 eV based on the commonly assumed value of −5.15 eV versus vacuum level for ferrocene/ferrocenium (Figure S1, Table S1).[16–18] Accordingly, similar to thienoacenes (HOMO ca. −5.5 eV)[19] and different to pentacene (HOMO ca. −5.0 eV) this fairly deep HOMO energy level suggests the possibility for air-stable *p*-channel operation of transistor devices based on **Ph_2ATTA**.

Single crystals suitable for X-ray structure analysis could be grown from a concentrated DMF solution by slow solvent evaporation. The monoclinic crystals of the space group $P2_1/c$ exhibit a hexagonal shape and can be grown to a size of several hundred micrometers (Figure S3, Table S2). In the crystal structure **Ph_2ATTA** shows an almost perfectly planar DA-substituted π-scaffold with a torsion angle between the D and A heterocyclic moieties of only 9° (Figure 2a). The molecules in the crystal structure arrange in centrosymmetric dimers with antiparallel dipole alignment and an unusually large π-π distance of 4.58 Å (Figure 2b). The formation of this centrosymmetric dimer unit can be attributed to electrostatic interactions arising from the significant ground state dipole moment. Whilst these interactions would typically bring the two π-systems to a much closer contact of about 3.3–3.6 Å,[8,9] here the sterical demands of the spatially closely located acceptor's *tert*-butyl as well as the two phenyl moieties of the donor enforce a larger distance. These individual dimer units, however, direct now as a "supramolecular synthon"[20] the successive built-up of the crystal lattice in a so far not observed packing pattern (Figure 2b,c): A tight π-contact with two additional neighboring molecules at a very close distance of only 3.36 Å is obtained by a lateral rotational displacement of stacked molecules both on the upper and the lower π-surface of the dimer. In this arrangement the dicyanovinyl group of one neighbor molecule is located on top of the thiophene donor unit and the thiophene donor unit of another neighbor molecule is located on top of the dicyanovinyl group of a given **Ph_2ATTA** molecule. Such close DA-π-contacts with two neighbor molecules on one π-face are enabled by the fact that the more bulky parts of the *tert*-butyl and phenyl groups are easily accommodated within the expanded dimer unit (Figure 2c, Figure S4). Also, whilst

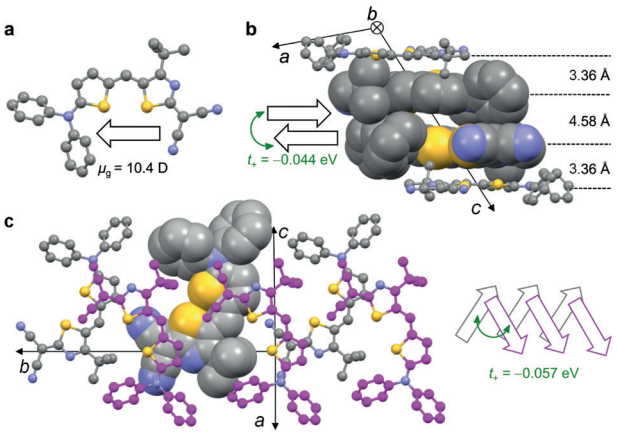

Figure 2. a) Chemical structure of merocyanine dye **Ph_2ATTA** in the single crystal and ground state dipole moment (μ_g). b) View along the *b*-axis of the unit cell of the crystal structure of **Ph_2ATTA**, indicating two distinct π-π distances, highlighted by representation in space filling view for antiparallel dimers. c) View on top of a dipolar zig-zag chain of six **Ph_2ATTA** molecules each with two close π-contacts to neighbor molecules (C: grey; N: blue, S: yellow). The carbon atoms of the upper three molecules are colored in magenta for better illustration of the overlap of molecules in the zig-zag chain. The transfer integrals t_+ (green arrows) determined by DFT calculations are given within b) the antiparallel dimer as well as for c) the zig-zag strand. For clarity, hydrogen atoms were omitted.

the resulting zig-zag-stack chain of dipolar molecules would lead to an electrostatically unfavored macrodipole, it is the centrosymmetric dimer unit that ensures an electrostatically favorable overall packing (for electrostatic potential map of various supramolecular units, see Figure S5). This quite interesting crystal structure of **Ph_2ATTA** can also be understood as a layer-like arrangement of dimers where each layer has a certain rotational displacement to provide the tight packing in the zig-zag-π-stacked strands (Figure S4). With regard to application of **Ph_2ATTA** as an organic semiconductor, the packing pattern with three close neighbor molecules appeared to be rather promising. This was further encouraged by DFT calculations[21] that afforded substantial hole-transfer integrals t_+ of −57 meV for the thiophene/dicyanovinyl contacts along the zig-zag chain and of −44 meV for the antiparallel dimer subunit (Figure 2b,c). These values are despite of the rather small contact surface for the thiophene/dicyanovinyl contact and the large distance for the dimer contact remarkably high and indeed in a similar range as those of prominent acene and thienoacene semiconductors.[19] Accordingly, promising percolation pathways are predicted along the one-dimensional zig-zag chain but also the interconnectivity to the next layer by the dimer unit is provided which should lead to percolation pathways throughout the crystal lattice of **Ph_2ATTA** in all directions.

To proof the suitability of **Ph_2ATTA** as an organic semiconductor, thin films of about 30 nm nominal thickness were processed either by spin-coating or by vacuum deposition onto substrates of Si/SiO_2 and $Si/SiO_2/AlO_x$/TPA, respectively (TPA: tetradecylphosphonic acid). Various substrate temperatures (T_{Sub}) were applied during deposition of

the active layer in vacuum as well as post-annealing steps for the spin-coated sample to optimize the transistor performance. Subsequently, gold electrodes were patterned via shadow mask technique to yield OTFTs in top-contact bottom-gate configuration (for further details see the Supporting Information). OTFT performance of vacuum- as well as solution-processed thin films of **Ph_2ATTA** (Figure 3, Figures S6 and S7) were all determined under ambient conditions for at least ten devices measured in the saturation regime with a source–drain voltage of $V_{DS} = -50$ V. The effective charge carrier mobilities μ and threshold voltages V_T were determined according to the equation $\mu = (2 I_{DS} L/[W C_i (V_{GS}-V_T)^2])$, where W denotes the width, L the length of the transistor channel and C_i the capacitance of the dielectric layer.

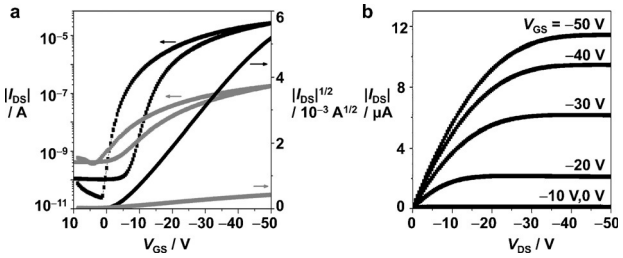

Figure 3. a) Transfer and b) output curves of bottom-gate, top-contact OTFTs of **Ph_2ATTA** vacuum-processed on TPA-modified $Si/SiO_2/AlO_x$ substrates (black, T_{Sub} at 70 °C) and spin-coated on Si/SiO_2 after annealing (gray, $CHCl_3$, 10^{-3} M, 3000 rpm, 30 minutes at 80 °C).

The solution-processed thin films exhibited moderate charge carrier mobilities of 0.0024 $cm^2 V^{-1} s^{-1}$ and a current on/off ratio (I_{on}/I_{off}) of 10^2–10^3 (Figure 3) after annealing of the active layer for 30 min at 80 °C, which is the highest reported value for solution-processed small dipolar molecules.[7] The vacuum-deposited layers showed even better values of 0.48 $cm^2 V^{-1} s^{-1}$ and an I_{on}/I_{off} of 10^6 which is the so far best performance realized for small dipolar organic semiconductor molecules. The effective mobility could be additionally enhanced by geometrical variations of W/L from a ratio of from 2 to 10 to afford a peak performance of up to 0.64 $cm^2 V^{-1} s^{-1}$ (Table S3). Unfortunately, this geometric variation is accompanied by a decrease of the current on/off ratio to 10^1–10^2 because of the increase in the off current (Table S3). All devices have reasonably low V_T values between −2 and −5 V as well as a small hysteresis (Figure 3, Figures S6 and S7).[6,7] Therefore for the first time a dipolar organic semiconductor enters the performance level known for benchmark organic semiconductor molecules such as pentacene ($\mu_h = 0.7$ $cm^2 V^{-1} s^{-1}$; $I_{on}/I_{off} = 10^8$).[22]

The morphology of **Ph_2ATTA** films was investigated by atomic force microscopy (AFM). AFM topography images for samples deposited from vacuum on TPA-modified substrates (Figure 4a, Figure S8) show large plate-like domains below smaller plates with sizes of about 1.5×2.1 μm^2. A layer-like structure can be clearly observed with an average individual layer thickness of about 1.7 ± 0.2 nm, ranging in the size of the crystallographic c-axis (1.8 nm). The topography of films from spin-coated samples displays more needle-like crystallites with smaller length between 100 to 300 nm, which is indicative for more disordered films, in accordance with the reduced device performance.

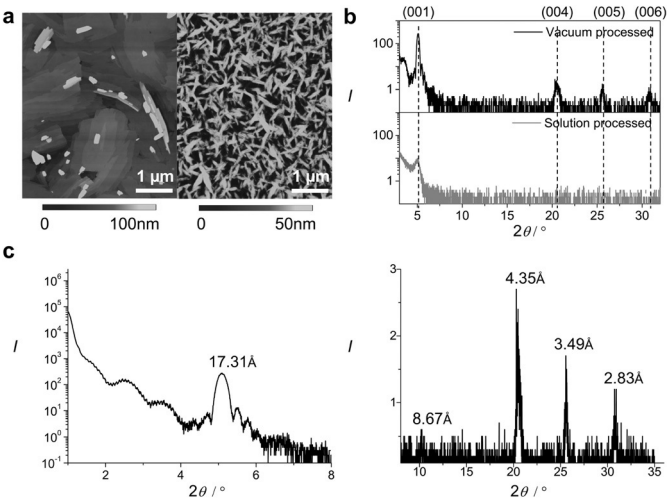

Figure 4. a) AFM height images of vacuum-processed thin-films of **Ph_2ATTA** on TPA-modified $Si/SiO_2/AlO_x$ substrates (left, $T_{Sub} = 70$ °C) and spin-coated on Si/SiO_2 after annealing (right, $CHCl_3$, 10^{-3} M, 3000 rpm, 30 min at 80 °C) with 30 nm nominal thickness (scale bars = 1 µm). b) Corresponding X-ray diffraction (XRD) patterns of vacuum- (top) and solution-processed (bottom) thin-films of **Ph_2ATTA**. c) Magnified XRD patterns of thin films of **Ph_2ATTA** deposited from vacuum on $Si/SiO_2/AlO_x$/TPA; small angle (left) and wide angle (right).

In order to further elucidate the orientation of the molecules within the active layer with respect to the substrate and to validate the same packing behavior as in the single crystal structure, out of plane X-ray diffraction (XRD) experiments of both films were performed. As shown in Figure 4b, XRD patterns of films processed in vacuum or from solution show similar diffraction patterns. As the solution-cast layer only exhibits one weak peak with low intensity we can conclude that the spin-coated film is less ordered compared to the better grown vacuum deposited one, despite thermal annealing. As shown in more detail in Figure 4c, peaks positioned at 5.10°, (10.20°,) 20.40°, 25.50° and 30.60° correspond to a d-spacing of 17.31 Å, (8.67 Å,) 4.35 Å, 3.49 Å, and 2.83 Å. The diffraction peaks are consistent with the calculated positions of the (001) diffractions deduced from a simulated XRD pattern based on the single crystal structure. The first diffraction at 5.10° with a d-spacing of about 17.31 Å is in good agreement with the observed layer heights of 1.7 ± 0.2 nm obtained by AFM cross-section analysis. Additionally, the Laue oscillations around the first Bragg reflection are evidence for a well-ordered film of high crystallinity, which is in accordance with the visual large domains observed by AFM. Under consideration of the single crystal structure, the observation of the (001) reflections suggests that **Ph_2ATTA** molecules lie flat on the substrate at a tilting angle relative to the substrate of only 25–30° (Figure S9). Such a face-on orientation of columnar stacks on the substrate, whilst highly desirable for organic photovoltaics (OPV),[23] is typically considered very unsuitable for

organic transistor devices where the current flow requires percolation pathways parallel to the substrate surface.[24] The latter is most commonly accomplished by tilted stacks of molecules that have an edge-on orientation to the substrate surface. Here, however, these percolation pathways are provided in an unusual way by the zig-zag chain motif and therefore the given packing of **Ph_2ATTA** should be indeed suitable for OTFT and OPV devices as well.

In conclusion, we introduced a new dipolar merocyanine dye **Ph_2ATTA** which adopts in the crystal structure as well as in vacuum- and solution-processed thin films a so far unprecedented packing arrangement built up from expanded antiparallel dimer units. These dimer synthons grow face-on on surfaces and exhibit an unusual zig-zag head-to-tail π-stack arrangement with close π-π-contacts of 3.36 Å laterally, providing percolation pathways for hole carriers parallel to the surface. This packing motif affords the so far highest ambient stable charge carrier mobility of 0.64 $cm^2V^{-1}s^{-1}$ in OTFTs fabricated from small dipolar organic semiconductor molecules which could be rationalized by the calculations of the transfer integrals and the high crystallinity of the films. Because of the interesting optical properties (strong absorption) and the suitable orientation of the transition dipoles parallel to the substrate these molecules might be promising for organic photovoltaic applications as well.

Keywords: crystal structures · dipole moments · donor–acceptor dyes · merocyanine dyes · organic thin-film transistors

How to cite: *Angew. Chem. Int. Ed.* **2015**, *54*, 10512–10515
Angew. Chem. **2015**, *127*, 10658–10661

[1] F. Würthner, K. Meerholz, *Chem. Eur. J.* **2010**, *16*, 9366–9373.
[2] H. Bürckstümmer, E. V. Tulyakova, M. Deppisch, M. R. Lenze, N. M. Kronenberg, M. Gsänger, M. Stolte, K. Meerholz, F. Würthner, *Angew. Chem. Int. Ed.* **2011**, *50*, 11628–11632; *Angew. Chem.* **2011**, *123*, 11832–11836.
[3] H.-W. Lin, S.-W. Chiu, L.-Y. Lin, Z.-Y. Hung, Y.-H. Chen, F. Lin, K.-T. Wong, *Adv. Mater.* **2012**, *24*, 2269–2272.
[4] S.-W. Chiu, L.-Y. Lin, H.-W. Lin, Y.-H. Chen, Z.-Y. Hung, Y.-T. Lin, F. Lin, Y.-H. Liu, K.-T. Wong, *Chem. Commun.* **2012**, *48*, 1857–1859.
[5] a) J. E. Anthony, *Angew. Chem. Int. Ed.* **2008**, *47*, 452–483; *Angew. Chem.* **2008**, *120*, 460–492; b) J. Mei, Y. Diao, A. L. Appleton, L. Fang, Z. Bao, *J. Am. Chem. Soc.* **2013**, *135*, 6724–6746; c) H. Dong, X. Fu, J. Liu, Z. Wang, W. Hu, *Adv. Mater.* **2013**, *25*, 6158–6183.
[6] L. Huang, M. Stolte, H. Bürckstümmer, F. Würthner, *Adv. Mater.* **2012**, *24*, 5750–5754.
[7] A. Liess, L. Huang, A. Arjona-Esteban, A. Lv, M. Gsänger, V. Stepanenko, M. Stolte, F. Würthner, *Adv. Funct. Mater.* **2015**, *25*, 44–57.
[8] F. Würthner, S. Yao, T. Debaerdemaeker, R. Wortmann, *J. Am. Chem. Soc.* **2002**, *124*, 9431–9447.
[9] A. Zitzler-Kunkel, M. Lenze, N. M. Kronenberg, A.-M. Krause, M. Stolte, K. Meerholz, F. Würthner, *Chem. Mater.* **2014**, *26*, 4856–4866.
[10] A. Ojala, PhD thesis, Universität Würzburg, **2012** (available via https://opus.bibliothek.uni-wuerzburg.de).
[11] F. Würthner, C. Thalacker, R. Matschiner, K. Lukaszuk, R. Wortmann, *Chem. Commun.* **1998**, 1739–1740.
[12] E. Ripaud, T. Rousseau, P. Leriche, J. Roncali, *Adv. Energy Mater.* **2011**, *1*, 540–545.
[13] A. Leliège, J. Grolleau, M. Allain, P. Blanchard, D. Demeter, T. Rousseau, J. Roncali, *Chem. Eur. J.* **2013**, *19*, 9948–9960.
[14] M. Watanabe, T. Yamamoto, M. Nishiyama, *Chem. Commun.* **2000**, 133–134.
[15] J. Wang, W.-F. Cao, J.-H. Su, H. Tian, Y.-H. Huang, Z.-R. Sun, *Dyes Pigm.* **2003**, *57*, 171–179.
[16] N. G. Connelly, W. E. Geiger, *Chem. Rev.* **1996**, *96*, 877–910.
[17] W. N. Hansen, G. J. Hansen, *Phys. Rev. A* **1987**, *36*, 1396–1402.
[18] C. M. Cardona, W. Li, A. E. Kaifer, D. Stockdale, G. C. Bazan, *Adv. Mater.* **2011**, *23*, 2367–2371.
[19] K. Takimiya, S. Shinamura, I. Osaka, E. Miyazaki, *Adv. Mater.* **2011**, *23*, 4347–4370.
[20] G. R. Desiraju, *Angew. Chem. Int. Ed. Engl.* **1995**, *34*, 2311–2327; *Angew. Chem.* **1995**, *107*, 2541–2558.
[21] ADF, 2013.01, Scientific Computing and Modelling NV, Amsterdam, **2013**.
[22] Y. Y. Lin, D. J. Gundlach, S. F. Nelson, T. N. Jackson, *IEEE Electron Device Lett.* **1997**, *18*, 606–608.
[23] C. Poelking, M. Tietze, C. Elschner, S. Olthof, D. Hertel, B. Baumeister, F. Würthner, K. Meerholz, D. Andrienko, *Nat. Mater.* **2015**, *14*, 434–439.
[24] S. Duhm, G. Heimel, I. Salzmann, H. Glowatzki, R. L. Johnson, A. Vollmer, J. P. Rabe, N. Koch, *Nat. Mater.* **2008**, *7*, 326–332.

Received: May 7, 2015
Published online: July 14, 2015

